A major purpose of the Technical Information Center is to provide the broadest dissemination possible of information contained in DOE's Research and Development Reports to business, industry, the academic community, and federal, state and local governments.

Although a small portion of this report is not reproducible, it is being made available to expedite the availability of information on the research discussed herein.

LA-UR--85-1256

DE85 010712

RECEIVED BY OSTI MAY 30 1985

Los Alamos National Laboratory is operated by the University of California for the United States Department of Energy under contract W-7405-ENG-36

TITLE: A FIRST COLLISION SOURCE METHOD FOR COUPLING MONTE CARLO AND DISCRETE ORDINATES FOR LOCALIZED SOURCE PROBLEMS

AUTHOR(S): Raymond E. Alcouffe

SUBMITTED TO. Joint Los Alamos/CEA Monte Carlo Conference, Cadarache, France April 1985.

DISCLAIMER

Los Alamos Los Alamos National Laboratory
Los Alamos, New Mexico 87545

A FIRST COLLISION SOURCE METHOD FOR COUPLING MONTE CARLO AND DISCRETE ORDINATES FOR LOCALIZED SOURCE PROBLEMS

Raymond E. Alcouffe
Radiation Transport Group, X-6
Los Alamos National Laboratory
Los Alamos, NM 87545

ABSTRACT

A difficult class of problems for the discrete-ordinates neutral particle transport method is to accurately compute the flux due to a spatially localized source. Because the transport equation is solved for discrete directions, the so-called ray effect causes the flux at space points far from the source to be inaccurate. Thus, in general, discrete ordinates would not be the method of choice to solve such problems! It is better suited for calculating problems with significant scattering. The Monte Carlo method is suited to localized source problems, particularly if the amount of collisional interactions is minimal. However, if there are many scattering collisions and the flux at all space points is desired, then the Monte Carlo method becomes expensive. To take advantage of the attributes of both approaches, we have devised a first collision source method to combine the Monte Carlo and discrete-ordinates solutions. That is, particles are tracked from the source to their first scattering collision and tallied to produce a source for the discrete-ordinates calculation. A scattered flux is then computed by discrete ordinates, and the total flux is the sum of the Monte Carlo and discrete ordinates calculated fluxes. In this paper, we present calculational results using the MCNP and TWODANT codes for selected two-dimensional problems that show the effectiveness of this method.

INTRODUCTION AND GENERAL CONSIDERATIONS

From time to time many people in the field of particle transport have become intrigued with the idea of somehow combining the attributes of the Monte Carlo method with those of the discrete-ordinates (or deterministic) method to some particular classes of problems. One hears such talk in the hallways or in offices, but not much has been presented in the formal literature; probably because most such combinations have been ad hoc and problem specific. Many times the linking has been done by hand[1] but there do exist some automated methods[2,3] for linking specific codes. We briefly summarize many of the ideas that have been used as follows:

GEOMETRIC LINKS

A geometric linking of the two methods has been by far the most popular consideration. The idea is that some problems naturally separate into at least two geometric regions; a perhaps geometrically complex source region and a geometrically simple deep penetration region. In such cases, it is natural to link the two methods through some boundary surface. Monte Carlo would transport through the geometrically complex region while discrete ordinates would transport from the boundary surface through the deep penetration region. This has been seen to be particularly advantageous when the Monte Carlo region has free-streaming paths while the discrete-ordinates region is dominated by scattering. This main job of the link is to tally the Monte Carlo results at the surface into a form that is usable by a discrete-ordinates code. In general, this would mean tallying into the correct energy, angle, and time bins for selected segments on the surface. The main assumption in this kind of geometric splitting is that there is little feedback through the splitting surface of one region upon the other. Otherwise, such a splitting would not make much sense.

In the reverse situation, instead of the Monte Carlo driving a discrete-ordinates calculation, the discrete-ordinates calculation can be used to generate a probability density function for the source of a subsequent Monte-Carlo calculation.[4] This source would also be at a splitting surface between two geometrical regions where the source region is geometrically simple and is readily treated by a discrete-ordinates method and the adjoining region is either geometrically complex or has free-streaming paths. Again the main the assumption is that there is little feedback through the splitting surface.

A last example is the use of a discrete ordinates adjoint calculation to set a spatial importance function for a particular problem to be solved by Monte Carlo. The problem would then be rerun in the Monte Carlo mode where splitting surfaces would be set according to the above generated importance function. Thus the discrete problem would be some kind of abstraction (simplification) of the actual Monte Carlo problem which provides the information to allow the Monte Carlo solution to be done much more efficiently. At least that is the goal of such methods.

ENERGY LINKS

In discrete-ordinates calculations, the spectral information is usually obtained from a multigroup approximation. For purposes of efficiency, the number of energy groups used is ≤ 100 while the remaining spectral detail is contained in the multigroup cross sections which are obtained from a representative weighting spectrum. As the number of groups used is decreased, the spectral information in the cross sections becomes more and more important. This spectral information is commonly obtained from representative infinite medium many group calculations. For complicated systems, 'representative' media are difficult to define so sometimes a continuous energy Monte-Carlo calculation is used to provide the spectral information which is utilized to form the multigroup cross sections. This procedure is economical only if many calculations on similar systems are envisioned.

We have discussed the basic ideas that people have used to link Monte Carlo and deterministic methods. This is by no means an exhaustive survey, but serves to give an idea of the considerations involved in this process. It seems that the possibilities are very numerous, but it is very difficult to quantify the criteria that would indicate the benefits of linking. In the following, we present a method which though not completely general, at least provides a systematic way of linking the two methods for problems where the source is quite localized.

DEVELOPMENT OF THE FIRST COLLISION METHOD

The first collision source method is a splitting of the problem based upon the nature of the source rather than on purely geometrical considerations. The main attribute of the source is that it is geometrically localized. The other aspect is that the problem is also collision dominated, although streaming regions may be included. From the Monte Carlo point of view, this problem is difficult because for various reasons, the solution is needed in all regions of space. From the discrete-ordinates point of view, the source is geometrically singular or, nearly so, resulting in severe ray effects which dominate the solution far from the source. These conditions are demonstrated in the results section below.

The first collision method is best described in an equation form. We write the original transport problem as,

$$\frac{1}{v}\frac{\partial \Psi}{\partial t} + \underline{\Omega} \cdot \nabla \psi(\underline{r},E,\underline{\Omega},t) + \sigma_t(\underline{r},E)\,\Psi(\underline{r},E,\underline{\Omega},t) =$$

$$\int_0^\infty dE' \sum_{\ell=0}^{L} (2\ell+1)\sigma_{s\ell}(\underline{r},E'\to E)\sum_{m=-\ell}^{\ell} Y_{\ell m}(\underline{\Omega})\,\phi_\ell^m(\underline{r},E',t) + Q(\underline{r},E,\underline{\Omega},t) \quad , \quad (1)$$

where $\Psi(\underline{r},E,\underline{\Omega},t)$ is the neutron flux defined such that $\hat{\underline{n}}\cdot\underline{\Omega}\,\Psi\,dEd\underline{\Omega}dSdt$ is the number of particles transported across a surface element dS with normal $\underline{n}$ at space point $\underline{r}$ in the energy range dE about E, in solid angle $d\underline{\Omega}$ about $\underline{\Omega}$ and

in the time interval dt about t; $\sigma_t(\underline{r},E)$ is the total cross section define such that $\sigma_t ds$ is the probability of having a collision in interval ds; $\sigma_{\ell s}(\underline{r},E'\to E)$ is the ℓth Legendre moment of the scattering transfer cross section, $Q(\underline{r},E,\underline{\Omega},t)$ is the source of particles at space point $\underline{r}$, with energy E, in direction $\underline{\Omega}$ at time t; $\phi_\ell^m(\underline{r},E,t)$ is the spherical harmonic of the angular flux, or

$$\phi_\ell^m(\underline{r},E,t) = \int_{4\pi} \psi(\underline{r},E,\underline{\Omega},t)\, Y_{\ell m}(\underline{\Omega})\, d\underline{\Omega} \ ;$$

$Y_{\ell m}(\underline{\Omega})$ are the spherical harmonics[4] normalized such that

$$\int Y_{\ell m}(\underline{\Omega})\, Y^*_{\ell m}(\underline{\Omega}) d\underline{\Omega} = \delta_{\ell\ell'}\, \delta_{mm'} \ .$$

To develop the method, we assume that the angular flux is written as

$$\psi(\underline{r},E,\underline{\Omega},t) = \psi_u(\underline{r},E,\underline{\Omega},t) + \psi_c(\underline{r},E,\underline{\Omega},t) \tag{2}$$

where ψ_u is the uncollided flux and ψ_c is the collided flux.

These fluxes satisfy the following equations:

$$\frac{1}{v}\frac{\partial \psi_u}{\partial t} + \underline{\Omega}\cdot\nabla\psi_u(r,E,\underline{\Omega},t) + \sigma_t(\underline{r},E)\,\psi_u(\underline{r},E,\underline{\Omega},t) = Q(\underline{r},E,\underline{\Omega},t) \tag{3}$$

$$\frac{1}{v}\frac{\partial \psi_c}{\partial t} + \underline{\Omega}\cdot\nabla\psi_c(\underline{r},E,\underline{\Omega},t) + \sigma_t(\underline{r},E)\,\psi_c(\underline{r},E,\underline{\Omega},t) = S_u(\underline{r},E,\underline{\Omega},t)$$

$$+ \int_0^\infty dE' \sum_{\ell=0}^{L} (2\ell+1)\sigma_{s\ell}(\underline{r},E'\to E) \sum_{m=-\ell}^{\ell} Y_{\ell m}(\underline{\Omega})\, \phi^m_{c\ell}(\underline{r},E',t) \tag{4}$$

where

$$S_u(\underline{r},E,\underline{\Omega},t) = \int_0^\infty dE' \sum_{\ell=0}^{L} (2\ell+1)\sigma_{s\ell}(\underline{r},E'\to E) \sum_{m=-\ell}^{\ell} Y_{\ell m}(\underline{\Omega})\, \phi^m_{u\ell}(\underline{r},E',t) \ .$$

It is seen that Eqs. (3) and (4) are equivalent to Eq. (1). Thus if the source Q is localized, then the split of Eqs. (3) and (4) provides a methodology for separating the problem solution into two parts. We can solve Eq. (3) by a method which treats the streaming from a localized source in an absorbing medium accurately, while we solve Eq. (4) with a method

which does a good job of treating collision dominated problems. We then obtain the total solution from Eq. (2).

Of course the problem description is not complete without specifying the boundary conditions and the initial conditions. If we designate a surface S that surrounds the calculational region of the problem, the general boundary conditions can be written as

$$\Psi(\underline{r}\epsilon S, E, \underline{\Omega}, t) = \Gamma(E, \underline{\Omega}, t) \text{ for } \hat{\underline{n}} \cdot \underline{\Omega} < 0 \tag{5}$$

to where $\hat{\underline{n}}$ is the outward normal to the surface. We can write the boundary conditions for Eqs. (3) and (4), respectively, as

$$\Psi_u(\underline{r}\epsilon S, E, \underline{\Omega}, t) = \Gamma(E, \underline{\Omega}, t) \quad \text{for } \underline{\Omega} \cdot \hat{\underline{n}} < 0 \tag{6}$$

$$\Psi_c(\underline{r}\epsilon S, E, \underline{\Omega}, t) = 0 \qquad \text{for } \underline{\Omega}, \hat{\underline{n}} < 0 \tag{7}$$

Thus the 'singularity' caused by the incident flux boundary condition is put into the uncollided problem while the collided problem has vacuum boundary conditions. The initial condition for Eq. (1) is written as $\Psi_u(\underline{r}, E, \underline{\Omega}, t_o) = \chi(\underline{r}, E, \underline{\Omega})$. Again for Eqs. (3) and (4), we write as initial conditions

$$\Psi_u(\underline{r}, E, \underline{\Omega}, t_o) = 0 \tag{8}$$

$$\Psi_c(\underline{r}, E, \underline{\Omega}, t_o) = \chi(\underline{r}, E, \underline{\Omega}) \tag{9}$$

although, in this case, the reasons for this split is not as clear cut as in the case of the boundary conditions and may be very problem dependent. This then completes the specification of the problem by what we have called the first collision method.

To further illustrate the method, we focus on Eq. (3) which has the form of a pure absorption problem driven by a known or given source with boundary conditions from Eq. (6) and an initial condition from Eq. (8). For simple geometries and sources, this equation can be solved analytically. For example, for a point source and a time independent problem, we have in cylindrical coordinates (ρ, z, μ, d),

$$\Psi(\underline{r}, E, \underline{\Omega}) = q(E)\delta(\phi)\delta\left(\mu - \frac{\rho}{\sqrt{\rho^2+(z-z_o)^2}}\right) \frac{e^{-\alpha(E, \underline{r}, \underline{r}_o)}}{\rho^2+(z-z_o)^2}$$

where

$$\alpha(E,\underline{r},\underline{r}_o) = \int_o^{\sqrt{\rho^2+(z-z_o)^2}} \sigma(E,s)ds$$

and the source is at the space point $(0,z_o)$.

For the more general case, the solution to Eq. (3) can be obtained by the method of ray tracing. This ray tracing may be accomplished in a variety of ways, either deterministically or by Monte Carlo. How the Monte Carlo may be carried out will be discussed in some detail below.

We solve Eq. (4) by the method of discrete ordinates. This method works well if the dominate sources in the problems are not localized or if it is scattering dominated. The method works poorly in free streaming, vacuum regions, or in pure absorbers with a localized source. Both types of problems usually give rise to the so-called ray effects. The results of the ray effect are locally very inaccurate values for the flux. This, of course, from the point of view of discrete ordinates, was the motivation for the split of Eqs. (3) and (4) in the first place. However, in some cases, the first collision source, u, itself may be quite localized and thus the solution to Eq. (4) will itself exhibit ray effects and will contaminate the solution to Eq. (3) which may be very accurate with inaccurate fluxes from Eq. (4). One can reason that for each energy, this effect will be the worst for a scattering ratio $c = \frac{\sigma_s}{\sigma_t} \simeq 0.5$. We will see that this effect is real by some examples in the next section.

In summary, we see that the first collision source method is conceptually very simple. It is best suited for problems which have regions in which the source is localized and imbedded in a collision dominated medium. It can thus be viewed as a ray effect mitigation method, although it may not always work well because of residual ray effects due to the fact that the first collision source itself may be quite localized. It seems to the author that the method is probably most useful for problems where the solution is to be obtained by discrete ordinates but that one employes an auxiliary method to help mitigate ray effects. We now investigate the consideration needed to solve Eq. (3) by the Monte Carlo method.

In the most general of situations, Eq. (3) can be solved as a Monte Carlo transport process in which particles are killed as soon as they make a collision. When we think about using a general code like MCNP[5] to set up the problem, we see that we immediately have available a very general geometric and energy description at our disposal. From the geometric point of view, the Monte Carlo method is solving the ray tracing problem. The most prominent characteristic of the problem is that we need tallies in spatial regions which correspond to the spatial mesh of the discrete-ordinates

calculations. This normally is an expensive process for general Monte Carlo calculations because it requires many collisions within each cell in order to obtain reliable statistics. However, because the particles are killed at each collision, it is most advantageous to employ an exponential transform which in effect follows each particle through its entire track from the source to the exterior boundary. This is in reality a deterministic ray tracing using the code to obtain the correct weighting along the track. In the MCNP code, we write the exponential transform as,

$$\sigma_{ex} = \sigma_t (1 - p\,\mu),$$

where

σ_{ex} is the transformed cross section,

σ_t is the true cross section,

p is the transform (stretching) parameters $|p|<|$,

μ is the cosine of the angle between a preferred direction and the particle direction.

The weight of the particle is given by,

$$W_{ex} = W \frac{e^{-p\sigma_t \mu s}}{1 - p\mu}$$

where

W_{ex} is the new weight,

W is the original weight.

This is very appropriate for a purely absorbing problem in that few particles will collide but will yield the correct contribution to the flux tally for each cell.

The accuracy of the method is further enhanced by doing a strategic source biasing in angle. The object here is to assure that sufficient cracks will go through each tally cell to obtain good statistics for that cell. This geometric source biasing is relatively easy to accomplish because we know a priori where our tally cells are and there is a one-to-one correspondence between the source angular emission and the angle of the track between the tally cell and the source. As an aside, after some thought, it is seen that there these processes can be readily vectorized because of their deterministic properties. This is not done in the MCNP code at present, but some

vectorization is slated for the future. At any rate, these biasing techniques can be used effectively to efficiently obtain the first collision source by Monte Carlo along with an estimate of the statistical error. In the following, we present a numerical example which illustrates the points discussed above.

SOME TYPICAL STEADY-STATE EXAMPLES IN R-Z GEOMETRY

The purpose of the section is to illustrate some of the points presented above and to indicate the usefulness of the Monte Carlo first-collision method in practical problems. All of the examples presented below are time-dependent and involve a mono-energetic, isotropic, point source in a two-dimensional cylinder. This type of problem, simple as it is, contains all of the necessary ingredients to illustrate the strong and weak points of the method. That is, a point source possesses an extreme example of singularity and the two dimensions will illustrate the ray effects of the discrete-ordinate calculation. Also by placing the point source on the axis of the cylinder, it is straightforward to obtain an analytic solution at each point in space and the zone (or mesh) average flux can be obtained by quadrature. This is very useful for assessing the accuracy of the Monte Carlo solution and for assessing the variance reduction strategies. The problem were run using the MCNP[5] and TWODANT[6] codes.

The first problem is a homogeneous cylinder with a point source at the center. The cylinder is 8 mfp high and has a 3 mfp radius. Since we have axial symmetry, we use a discrete ordinates spatial mesh of 10 x 12 equally spaced intervals in the r and z directions, respectively, with a reflecting boundary condition at the cylinder mid-plane. In the following solutions, we vary the scattering ratio using three values, c=0, 0.5, 1.0. The Monte Carlo solution of Eq. (3) is accomplished with MCNP unmodified. The tallies are made using the track length estimator for the flux in tally cells which correspond to the discrete-ordinates mesh, 120 volumes in this instance. We use this as exponential transform stretching parameter of 0.9 and we exponentially bias the source sampling with a parameter of 3.4. This directs more particles upward along the axis of the cylinder. We run the Monte Carlo problem until the error estimate in each cell is down to a few percent. In Figs. 1 and 2, we present the results of three calculations for the uncollided flux, one analytic, and two Monte Carlo. In Fig. 1, we show the zone average flux along the top row of cells of the cylinder and in Fig. 2, we show the zone average flux along the outside column of cells. The two Monte Carlo runs contain approximately 90,000 and 170,000 histories, respectively. The greatest discrepancy that we see is at the top near the axis of the cylinder in which not enough particles have contributed to the scores there in the 90,000 case. By 170,000 histories, we have results which almost reproduce the analytic solution. By way of reference to accuracy, we show in Figs. 3 and 4 three calculations, one analytic and two discrete ordinates, S4 and S16, respectively. We immediately see how devastating the ray effects are even for the relatively small problem. Incidentally, S4 consists of 24 discrete angles spread approximately uniformly over the unit sphere while S16 has 288 discrete angles. Thus the errors in either Monte Carlo calculation are minor in comparison with these.

Our next calculation will serve to illustrate two things; the effect of the Monte Carlo first collision source errors upon the solution with scattering, and the effect of innaccuracies in the discrete ordinates part of the calculation upon the total solution. In Figs. 5 and 6, we present the zone flux for problems with scattering ratios of 0.5 and 1.0 computed with the two Monte Carlo first-collision sources and the analytic first-collision source. It is seen that there is some effect due to the different Monte Carlo calculations in the c = 0.5 case, but there are different discrepancies, and as expected they do not even show up in the c = 1 case. Again we contrast these errors with those induced by the discrete ordinates part of the calculation as shown in Figs. 7 and 8 for c = 0.5 and c = 1. There we depict S4 and S16 calculations with the analytic first collision source and, for reference, the Monte Carlo 170,000 history first-collision source with S16 discrete ordinates. The oscillations are due to ray effects in the Sn part of the calculation, but these oscillations are mitigated from those occurring in normal Sn calculations as can be seen from Figs. 9 and 10. In Fig. 9, we present the calculations for c = 0.5 for the first collision and the normal S16 versions and, one, can see that the oscillations have indeed been mitigated in the first-collision case. In Fig. 10 we present similar results for c = 1 and S4 and, we see that even in this case, there is some residual effect of ray effects for the normal S4. Thus, returning to Figs. 7 and 8, we see that we have not eliminated errors due to ray effects for problems with some scattering, but we have succeeded in greatly mitigating the errors. For example, comparing Figs. 7 and 9, we see that the first collision S4 for c = 0.5 is much better than the normal S16 calculation. As we indicated above, the c = 0.5 case has the largest errors for the first-collision method so this gives an idea of what benefits can be obtained by employing it.

CONCLUSIONS AND RECOMMENDATIONS

We have outlined a general Monte Carlo based first-collision source method of performing transport calculations in problems involving a highly geometrically localized source in a scattering medium. We have illustrated the benefits of the procedure in a series of simple problems which nevertheless contain the essential ingredients for making our point. This shows how badly the normal discrete-ordinates method usually does for problems in which the scattering ratio is $\lesssim 0.5$. We have briefly examined what the Monte Carlo considerations are and have compared the Monte Carlo generated first-collision zone fluxes with those generated from an analytical approach. This shows that statistical errors do have an effect, but, as the scattering in the problem increases, these effects seem to be minor compared with the errors generated in the discrete ordinates part of the problem as long as the Monte Carlo sampling in each spatial cell is adequate.

It has become apparent that the Monte Carlo efficiency can be greatly improved by doing some fairly simple things and one that is not so simple. Of most benefit would be to more carefully do the source angle biasing so that all spatial cells will be equally covered by particle tracks. This assumes that the exponential transform is also used so that the partial tracks are followed until the outside boundary of the problem is reached. These sorts of considerations are relatively simple to implement. Since the Monte Carlo

involves no scattering, then the whole procedure is straightforwardly vectorized. This, however, is not so simple to do but the payoff in computational time would be worth it.

As we think of the more general time-dependent case with more complicated sources, we can well see that there is a great advantage to having a discrete-ordinate calculation enhanced by the Monte Carlo first-collision procedure. From the discrete-ordinates point-of-view, the implementation is easy and very convenient and should help to relieve many of the knotty problems involved in multidimensional, time-dependent problems. From the Monte Carlo pont-of-view, the question arises, why not just do the whole problem by Monte Carlo? In some cases this might indeed be best; but if a full vectorized first-collision method is available and the problem requires that the solution be obtained in all regions of its geometry and there are many scattering collisions which take place, then this linking with discrete ordinates will be highly advantageous and efficient.

REFERENCES

1. W. T. Urban, T. J. Seed, D. J. Dudziak, "Coupled Monte Carlo/Discrete-Ordinates Calculations for ETF Vacuum-Pumping Duct Shielding," Trans. Am. Nucl. Soc., 39, (1981).

2. M. B. Emmett, C. E. Burgart, T. J. Hoffman, "DOMINO - A General Purpose Code for Coupling Discrete Ordinates and Monte Carlo Radiation Transport Calculations," Oak Ridge National Laboratory Report, ORNL-4853 (1973).

3. M. B. Emmett, "The MORSE Monte Carlo Radiation Transport System," Oak Ridge National Laboratory Report, ORNL-4972 (1975).

4. John D. Jackson, Classical Electrodynamics, p. 64, John Wiley & Sons, Inc., New York.

5. LASL Group X-6, "MCNP - A General Monte Carlo Code for Neutron and Photon Transport," LA-7396-M, revised (1981).

6. R. E. Alcouffe, F. W. Brinkley, D. R. Marr, R. D. O'Dell, "User's Guide for TWODANT: A Code package for Two-Dimensional, Diffusion Accelerated, Neutral-Particle Transport," LA-10049-M, rev. 1 (1984).

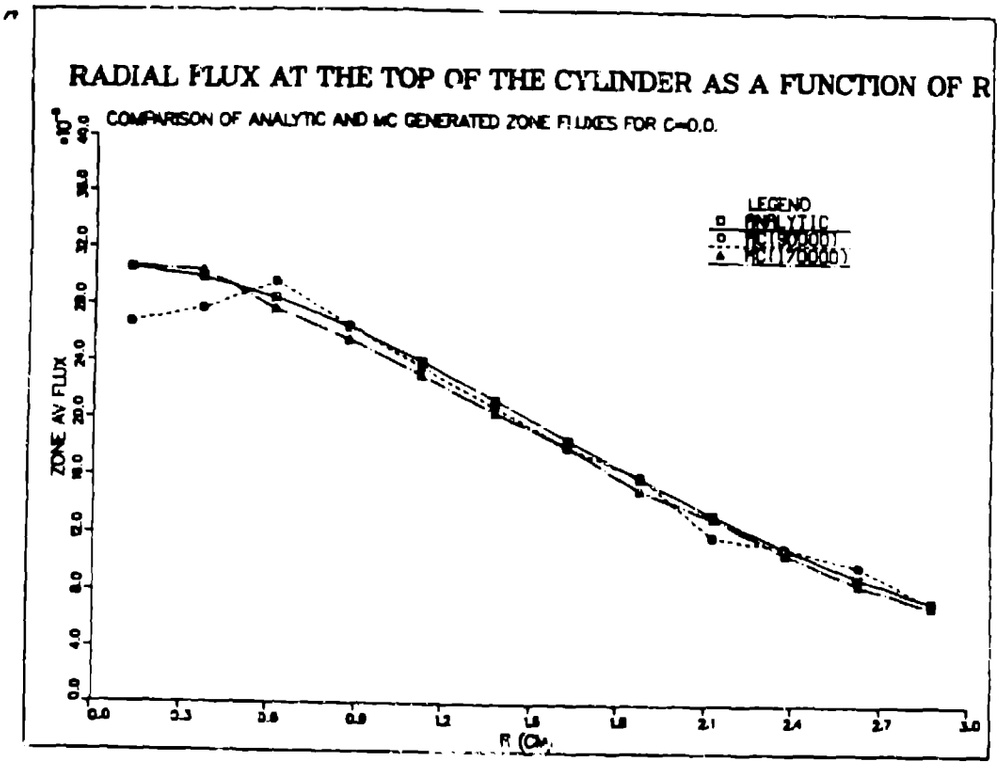
RADIAL FLUX AT THE TOP OF THE CYLINDER AS A FUNCTION OF R
COMPARISON OF ANALYTIC AND MC GENERATED ZONE FLUXES FOR C=0.0.
LEGEND
ANALYTIC
MC(900000)
MC(1700000)
ZONE AV FLUX
R (CM)

Fig. 1

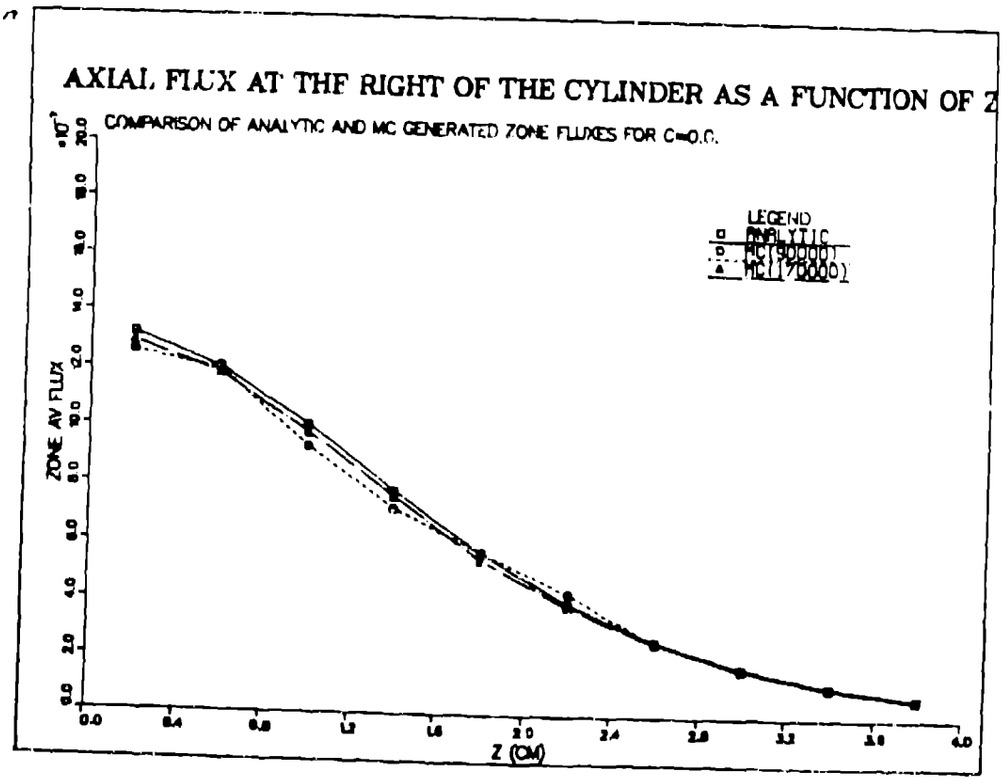
AXIAL FLUX AT THE RIGHT OF THE CYLINDER AS A FUNCTION OF Z
COMPARISON OF ANALYTIC AND MC GENERATED ZONE FLUXES FOR C=0.0.
LEGEND
ANALYTIC
MC(900000)
MC(1700000)
ZONE AV FLUX
Z (CM)

Fig. 2

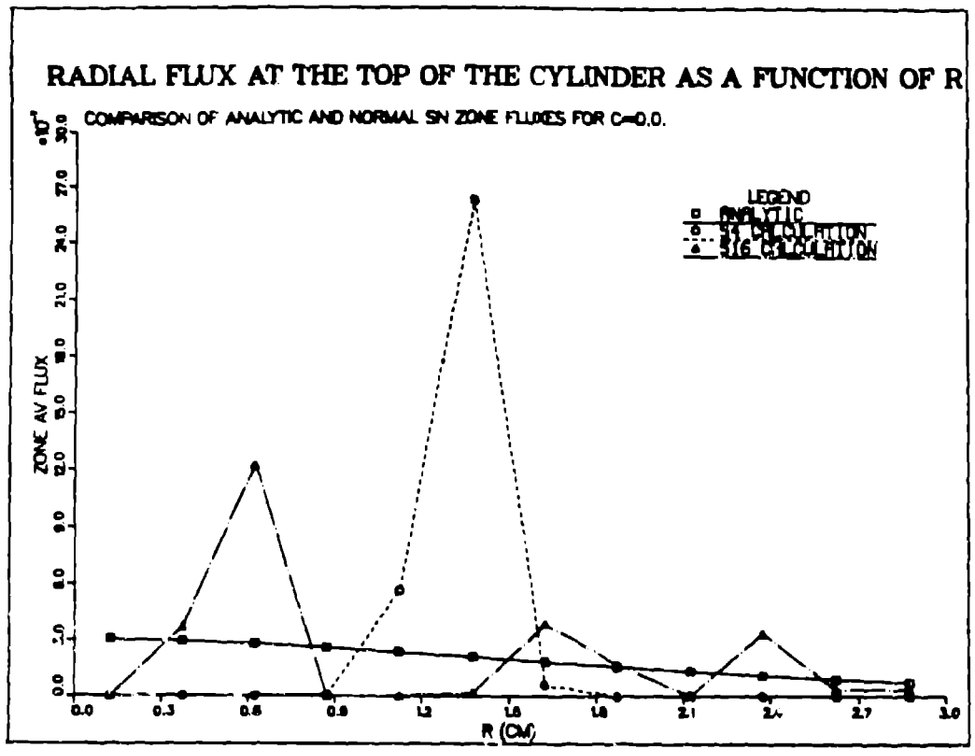
RADIAL FLUX AT THE TOP OF THE CYLINDER AS A FUNCTION OF R
COMPARISON OF ANALYTIC AND NORMAL SN ZONE FLUXES FOR C=0.0.
LEGEND
ANALYTIC
S4 CALCULATION
S16 CALCULATION
ZONE AV FLUX
R (CM)

Fig. 3

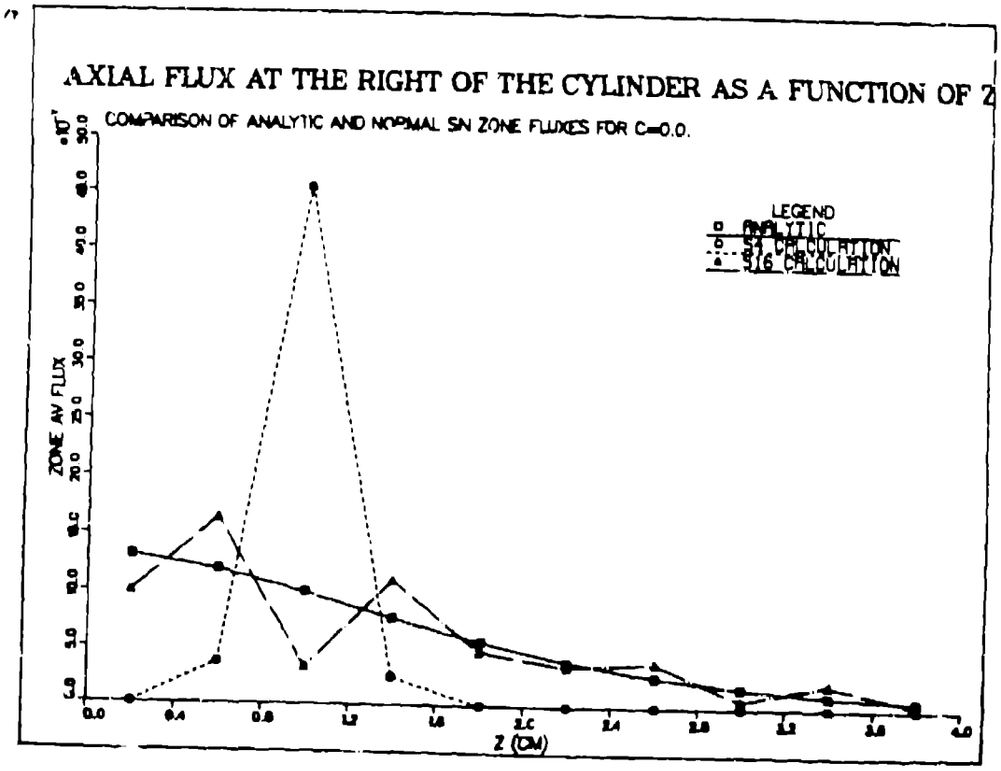
AXIAL FLUX AT THE RIGHT OF THE CYLINDER AS A FUNCTION OF Z
COMPARISON OF ANALYTIC AND NORMAL SN ZONE FLUXES FOR C=0.0.
LEGEND
ANALYTIC
S4 CALCULATION
S16 CALCULATION
ZONE AV FLUX
Z (CM)

Fig. 4

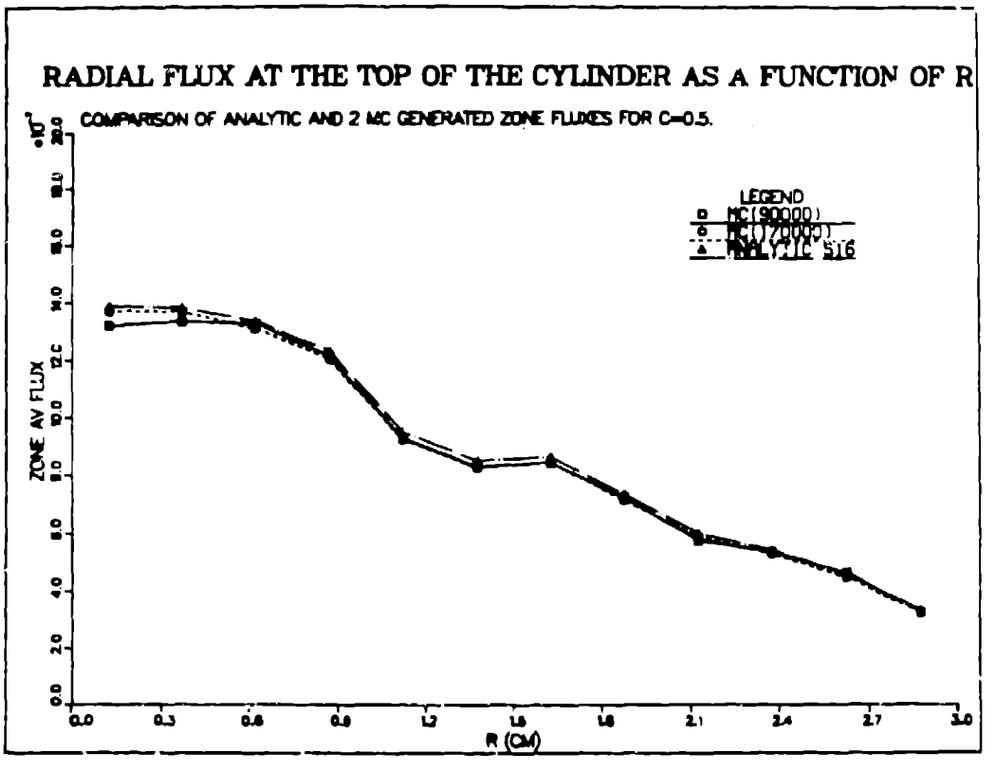
RADIAL FLUX AT THE TOP OF THE CYLINDER AS A FUNCTION OF R
COMPARISON OF ANALYTIC AND 2 MC GENERATED ZONE FLUXES FOR C=0.5.
LEGEND
ZONE AV FLUX
R (CM)

Fig. 5

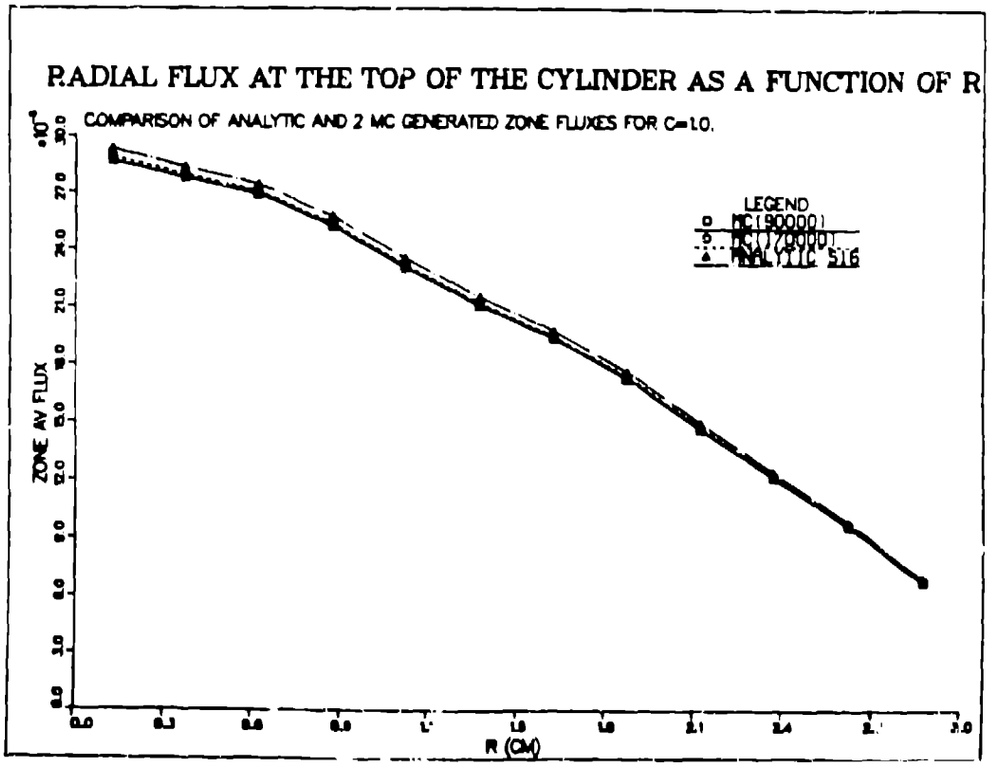
RADIAL FLUX AT THE TOP OF THE CYLINDER AS A FUNCTION OF R
COMPARISON OF ANALYTIC AND 2 MC GENERATED ZONE FLUXES FOR C=1.0.
LEGEND
ZONE AV FLUX
R (CM)

Fig. 6

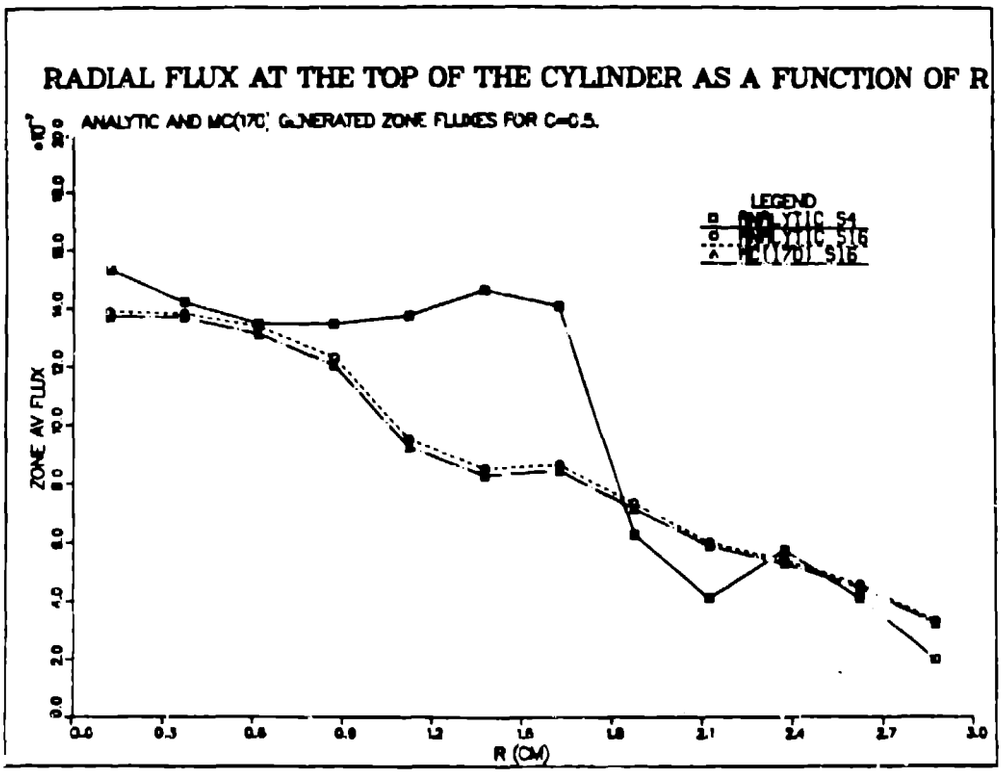
RADIAL FLUX AT THE TOP OF THE CYLINDER AS A FUNCTION OF R
ANALYTIC AND MC(170) GENERATED ZONE FLUXES FOR C=0.5.
LEGEND
ZONE AV FLUX
R (CM)

Fig. 7

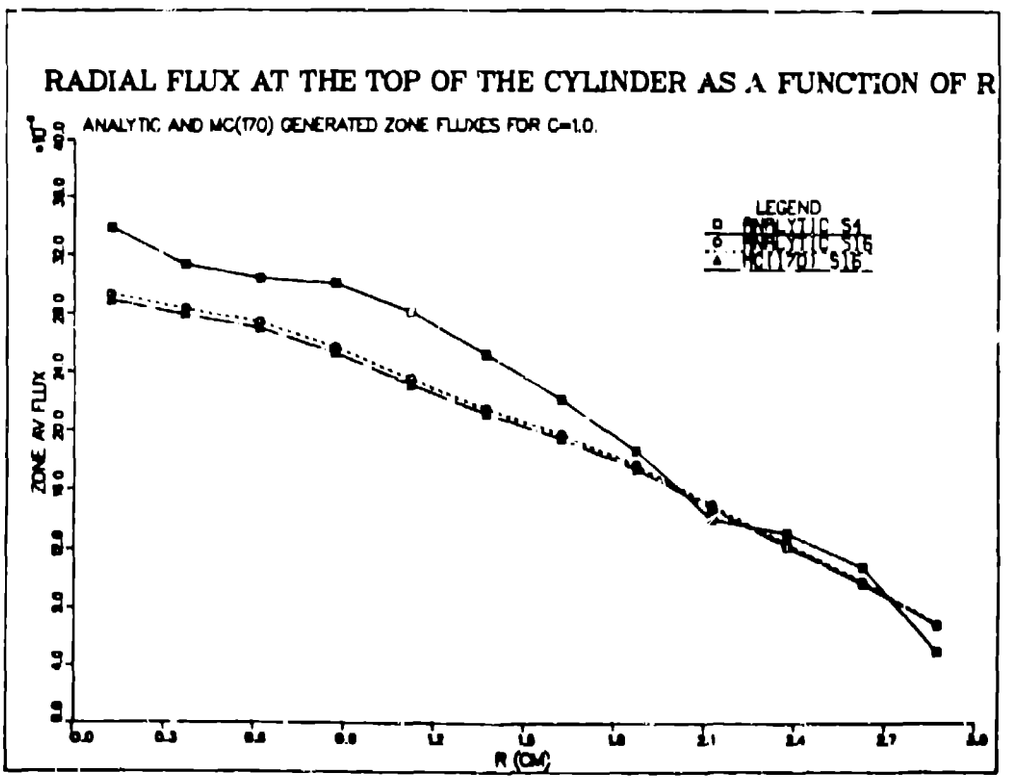
RADIAL FLUX AT THE TOP OF THE CYLINDER AS A FUNCTION OF R
ANALYTIC AND MC(170) GENERATED ZONE FLUXES FOR C=1.0.
LEGEND
ZONE AV FLUX
R (CM)

Fig. 8

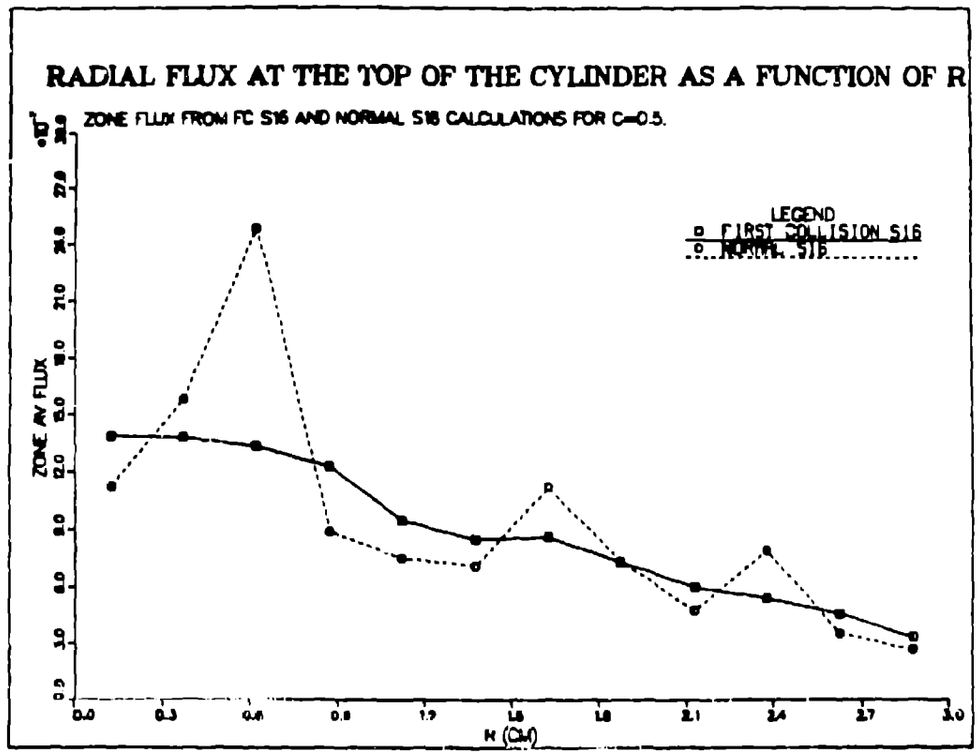
RADIAL FLUX AT THE TOP OF THE CYLINDER AS A FUNCTION OF R
ZONE FLUX FROM FC S16 AND NORMAL S16 CALCULATIONS FOR C=0.5.
LEGEND
FIRST COLLISION S16
NORMAL S16
ZONE AV FLUX
R (CM)

Fig. 9

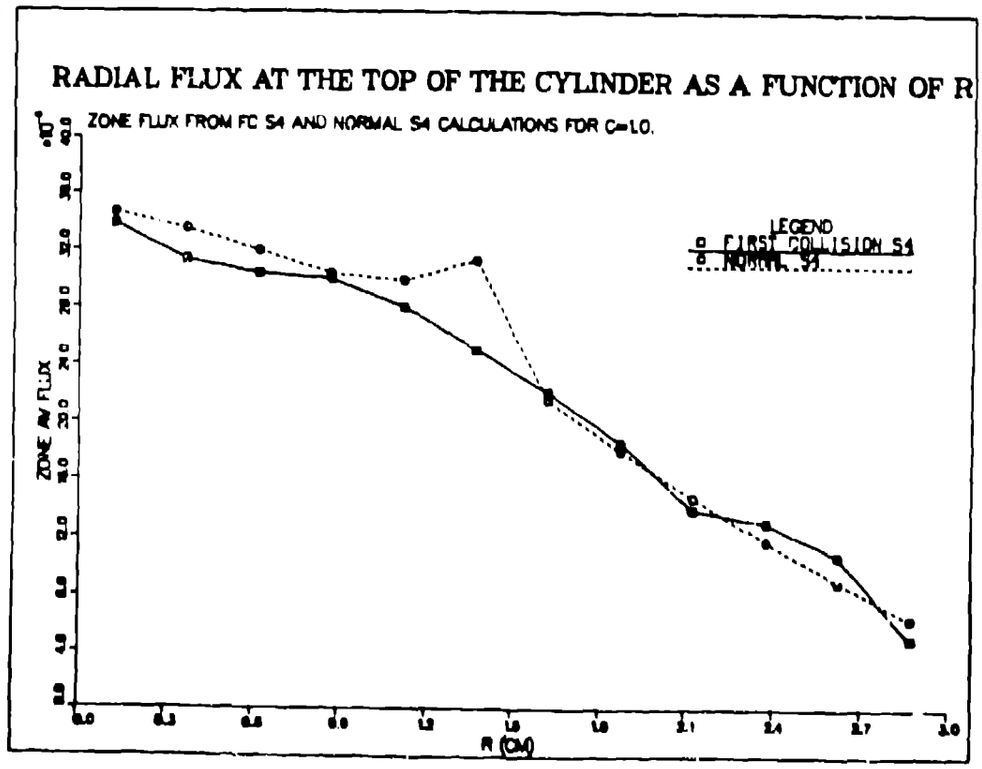
RADIAL FLUX AT THE TOP OF THE CYLINDER AS A FUNCTION OF R
ZONE FLUX FROM FC S4 AND NORMAL S4 CALCULATIONS FOR C=1.0.
LEGEND
FIRST COLLISION S4
NORMAL S4
ZONE AV FLUX
R (CM)

Fig. 10